Gazi Üniversitesi
Fen Bilimleri Dergisi
PART C: TASARIM VE TEKNOLOJİ

Gazi University
Journal of Science
PART C: DESIGN AND TECHNOLOGY

GU J Sci, Part C, 12(1): 1-16 (2024)

Flow Properties of An Ahmed Body with Different Passive Flow Control Methods

Kemal KOCA[1,2,*], Mustafa ÖZDEN [3]

[1]*Abdullah Gül University, Engineering Faculty, Department of Mechanical Engineering, Kayseri, Türkiye*

[2]*Abdullah Gül University, Engineering Faculty, Department of Mechanical Engineering, KOCA Research Group, Kayseri, Türkiye*

[3]*Clemson University, Department of Electrical and Computer Engineering, Real-Time Control and Optimization Laboratory, Clemson, USA*

Article Info

Research article
Received: 26/07/2023
Revision: 13/10/2023
Accepted: 08/11/2023

Keywords

Ahmed Body
Vehicle aerodynamics
Passive flow control
Drag reduction
FloEFD

Makale Bilgisi

Araştırma makalesi
Başvuru: 26/07/2023
Düzeltme: 13/10/2023
Kabul: 08/11/2023

Anahtar Kelimeler

Ahmed Body
Araç aerodinamiği
Pasif akış kontrolü
Sürükleme azaltımı
FloEFD

Graphical/Tabular Abstract (Grafik Özet)

The flow topology created on the slant surface and wake region of an Ahmed Body with and without passive flow control strategies was investigated using a numerical simulation using the FloEFD program. / Pasif akış kontrol stratejileri olan ve olmayan bir Ahmed Cisminin eğimli yüzeyi ve iz bölgesi üzerinde oluşturulan akış topolojisi, FloEFD programı kullanılarak sayısal bir simülasyon kullanılarak incelenmiştir.

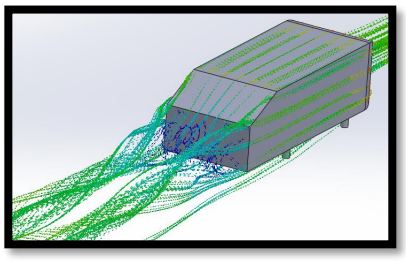

***Figure A**: The flow topology formed around Ahmed Body / **Şekil A:** Ahmed Gövdesi etrafında oluşan akış topolojisi*

Highlights (Önemli noktalar)

- *Numerical findings clearly demonstrated that the best performance in terms of drag reduction was achieved when spherical and hemispherical flow control techniques were applied at the rear of the inclined surface of the Ahmed Body. / Sayısal bulgular, sürükleme azaltımı açısından en iyi performansın, Ahmed Gövdesinin eğimli yüzeyinin arka kısmında küre ve yarı küresel şekilli akış kontrol teknikleri uygulandığında elde edildiğini açıkça ortaya koymuştur.*
- *Spherical and semi-spherical shaped flow controllers positioned at the rear of the inclined surface resulted in friction reductions of 6% and 7%, respectively. / Eğimli yüzeyin arka kısmında konumlandırılan küresel ve yarı küresel şekilli akış kontrolörleri, sırasıyla %6 ve %7 oranında sürtünme azalmasına neden olmuştur.*

***Aim (Amaç):** The objective of this study is to investigate the flow features formed around Ahmed Body and to apply the passive control methods so as to achieve less drag coefficient. / Bu çalışmanın amacı, Ahmed Cismi çevresinde oluşan akış özelliklerini araştırmak ve daha az direnç katsayısı elde etmek için pasif kontrol yöntemlerini uygulamaktır.*

***Originality (Özgünlük):** Different passive control techniques employed on surface of Ahmed Body at the first time in the literature and it was also first time to utilize FloEFD software in the field of vehicle aerodynamic. / Literatürde ilk kez Ahmed Gövdesinin yüzeyinde farklı pasif kontrol teknikleri kullanılmış ve aynı zamanda FloEFD yazılımından araç aerodinamiği alanında da ilk kez yararlanılmıştır.*

***Results (Bulgular):** The FloEFD numerical findings clearly pointed out that the flow controllers with spherical and semi-spherical shapes placed behind the angled surface reduced friction by 6% and 7%, respectively. / FloEFD sayısal bulguları, açılı yüzeyin arkasına yerleştirilen küresel ve yarı küresel şekilli akış kontrolörlerinin sürtünmeyi sırasıyla %6 ve %7 oranında azalttığını açıkça ortaya koydu.*

***Conclusion (Sonuç):** Consequently, it was pronouncedly seen that different passive control methods enabled of having less drag forces on the Ahmed Body. Further, this was proved with the FloEFD numerical results as well as literature findings. / Sonuç olarak, farklı pasif kontrol yöntemlerinin Ahmed Cismi üzerinde daha az sürükleme kuvveti oluşturmasına olanak sağladığı açıkça görülmüştür. Ayrıca bu durum FloEFD sayısal sonuçlarının yanı sıra literatür bulgularıyla da kanıtlanmıştır.*

*Corresponding author, e-mail: kemal.koca@agu.edu.tr
DOI: 10.29109/gujsc.1333049

GU J Sci, Part C, 12(1): 1-16 (2024)

Gazi Üniversitesi
Fen Bilimleri Dergisi
PART C: TASARIM VE TEKNOLOJİ

Gazi University
Journal of Science
PART C: DESIGN AND TECHNOLOGY

http://dergipark.gov.tr/gujsc

Flow Properties of An Ahmed Body with Different Passive Flow Control Methods

Kemal KOCA[1,2,*], Mustafa ÖZDEN [3]

[1]*Abdullah Gül University, Engineering Faculty, Department of Mechanical Engineering, Kayseri, Türkiye*

[2]*Abdullah Gül University, Engineering Faculty, Department of Mechanical Engineering, KOCA Research Group, Kayseri, Türkiye*

[3]*Clemson University, Department of Electrical and Computer Engineering, Real-Time Control and Optimization Laboratory, Clemson, USA*

Article Info

Research article
Received: 26/07/2023
Revision: 13/10/2023
Accepted: 08/11/2023

Keywords

Ahmed Body
Vehicle aerodynamics
Passive flow control
Drag reduction
FloEFD

Abstract

A numerical simulation by utilizing the FloEFD software was carried out in order to investigate the flow topology formed on slant surface and wake region of an Ahmed Body with and without passive flow control techniques. The effects of those flow controllers on flow at the slant surface and wake region by influencing the flow topology as well as aerodynamic drag coefficient examined carefully. The numerical findings clearly revealed that the best performance in terms of providing the drag reduction obtained when sphere and hemispherical shape flow control techniques were applied at the rear part of slant surface of Ahmed Body. Sphere and hemispherical shape flow controllers positioned at the rear part of slant surface led to have drag reduction of 6% and 7%, respectively. Besides, the results of current study compared with the results obtained from published studies in the literature. It was clearly observed that they are consistent with each other even though they were found by different software.

Ahmed Gövdesinin Farklı Pasif Akış Kontrol Yöntemleriyle Akış Özellikleri

Makale Bilgisi

Araştırma makalesi
Başvuru: 26/07/2023
Düzeltme: 13/10/2023
Kabul: 08/11/2023

Anahtar Kelimeler

Ahmed Body
Araç aerodinamiği
Pasif akış kontrolü
Sürükleme azaltımı
FloEFD

Öz

Ahmed Gövdesinin eğimli yüzeyinde ve iz bölgesinde oluşan akış topolojisini pasif akış kontrol teknikleri ile ve pasif akış kontrol teknikleri olmadan incelemek amacıyla FloEFD yazılımı kullanılarak sayısal bir simülasyon gerçekleştirilmiştir. Bu akış kontrolörlerinin akış topolojisini ve aerodinamik sürükleme katsayısını etkileyerek eğik yüzey ve iz bölgesindeki akış üzerindeki etkileri dikkatle incelenmiştir. Sayısal bulgular, sürükleme azaltımı açısından en iyi performansın, Ahmed Gövdesinin eğimli yüzeyinin arka kısmında küre ve yarı küresel şekilli akış kontrol teknikleri uygulandığında elde edildiğini açıkça ortaya koymuştur. Eğimli yüzeyin arka kısmında konumlandırılan küresel ve yarı küresel şekilli akış kontrolörleri, sırasıyla %6 ve %7 oranında sürtünme azalmasına yol açtı. Ayrıca mevcut çalışmanın sonuçları literatürde yayınlanmış çalışmalardan elde edilen sonuçlarla karşılaştırılmıştır. Farklı yazılımlarla bulunsalar da birbirleriyle tutarlı oldukları açıkça görüldü.

1. INTRODUCTION (GİRİŞ)

Enhancing the aerodynamic performance of automobiles especially by reducing the drag forces are important assignments in fluid mechanics community. Those aerodynamic drag forces primarily form at the rear part and blunt nose of vehicles owing to formation of large separation flows. Additionally, the design constraint necessitates body bluffness, which in turn necessitates complex three-dimensional flow in the afterbody. Therefore, drag reduction methods on conventional aerodynamic cars have recently become of great interest to automakers because they are more repeatable and offer a better understanding of fuel usage to safeguard the environment globally.

Ahmed body was developed by Ahmed et al. [1] and it became a forerunner example for aerodynamic researchers. Similar to concept of crucial geometries presented by Morel [2], along with other bodies such as slanted cylinders, the Ahmed body is considered a crucial geometry [3]. To date, various experimental techniques have been performed on strategies including (*i*) active, (*ii*) passive, or (*iii*) a combination of (*i*) & (*ii*) control techniques for

*Corresponding author, e-mail: kemal.koca@agu.edu.tr
DOI: 10.29109/gujsc.1333049

obtaining drag reduction on universal vehicle geometries to gain crucial understanding on the relationship between the pressure drag generation and the complex wake structure [4-6]. The study performed by Bellman et al. [7] clearly revealed that fuel consumption could be reduced by 5% when the aerodynamic drag of ground vehicles decreased by 10%. Active drag reduction methods such as performing synthetic jet actuation [8], employing pulsed jets [9], utilizing steady blowing [10], considering a combination of suction and blowing [11] exhibited extraordinary performance by affecting the wake behind the Ahmed body. However, it could be said that active ones recently have lag behind passive drag reduction methods since the passive ones are comparatively easier to fabricate and enforce. Those techniques consisted of deflector plates [12], contoured transverse grooves [13], vortex generators (VGs) [14]. In addition to extra component, the drag reduction could be performed with geometric modification such as afterbody rounding [15], body cavity [16]. Table 1 covers previous research at low Reynolds numbers belonging to the Ahmed Body.

The novelty of the paper was twofold, (*i*) V_2 and V_3 were investigated in the first time in the literature with these dimensions and (*ii*) Besides numerical attempt with ANSYS taken place literature, it was the first time that FloEFD software was utilized, and the results were compared with ANSYS's results taken place in the literature. The aforementioned factors have prompted this work's objective, which is to clarify the aerodynamic performance of several passive flow control varieties on the Ahmed Body. The rest of paper was arranged as follows: Section 2 identified the material and methods including numerical model, numerical method, and aerodynamic forces. The detailed results were presented in Section 3. The crucial findings were discussed and concluded by comparing the between each other in Section 4.

2. MATERIAL AND METHODS (MATERYAL VE METOD)

2.1. Numerical Model (Sayısal Model)

In this study, the dimensions of the geometries (according to the baseline model) were shown as in Figure 1. The total length of Ahmed Body was 1044 mm. The radius of rounded front part was 100 mm. Moreover, slant angle was selected as 25°. Related to the computational domain as illustrated in Figure 2, the front part of Ahmed Body was positioned 5L away from the domain inlet (L was length of Ahmed Body) and distance from the rear surface to the outlet of domain was 10L. According to the experience of previous studies of current authors [29-31], 10L was enough to see and investigate flow structures occurred at the wake of Ahmed Body. The ground of the computational domain was applied as no-slip condition. Symmetric conditions were applied at both side boundaries and at the top boundary. Both side boundaries were located 5D (D was width of Ahmed Body) away from the Ahmed Body. The inflow velocity coming from the inlet was 40 m/s.

Table 1. Summary of low Reynolds number scaled model experiments over the Ahmed body (Ahmed cismi üzerinde düşük Reynolds sayısı ölçekli model deneylerinin özeti)

Method	Model scale	Reynolds Num.	Slant Angle	Reference
Numerical	1	8322	25°	[17]
Numerical	1/5.33	14000	0°	[18]
Experimental	1/4	14000	25°, 35°	[19]
Experimental	1/4	26000	25°	[20]
Experimental	1/5.3	17000	0°, 25°, 35°	[21]
Exp.+Num.	1/4	14800	25°	[22]
Numerical	1/0.288	8275	0°	[23]
Exp.+Num.	1/4	14800	25°	[24]
Numerical	1	10000	0°	[25]
Experimental	1/0.25	17000	0°	[26]
Experimental	1/4	14800	25°, 30°, 35°	[27]
Experimental	1/11	340, 410	0°	[28]

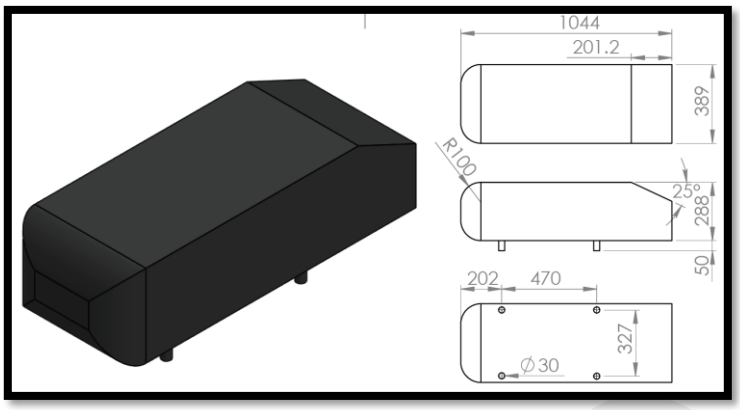

Figure 1. Technical sketch and dimensions of Ahmed body (baseline model), dimensions in mm (Ahmed gövdesinin teknik çizimi ve boyutları (temel model), mm cinsinden boyutlar)

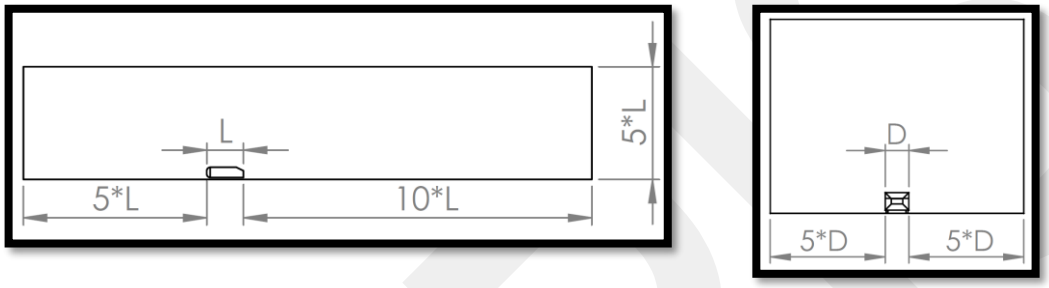

Figure 2. A schematic of computational domain, dimensions in mm (Hesaplama alanının şeması, boyutlar mm cinsindendir)

The simulation employed three-dimensional continuity and momentum equations-based on the finite volume method. The discretized algebraic equations were solved using bounded second-order implicit time. The general form of the Continuity and Momentum equations can be presented as:

$$\frac{\partial V_x}{\partial x}+\frac{\partial V_y}{\partial y}+\frac{\partial V_z}{\partial z}=0 \quad (1)$$

$$\rho\left(\frac{\partial V_x}{\partial \tau}+V_x\frac{\partial V_x}{\partial x}+V_y\frac{\partial V_x}{\partial y}+V_z\frac{\partial V_x}{\partial z}\right)=-\frac{\partial P}{\partial x}+\frac{\partial}{\partial x}\left[(\mu+\mu_t)\frac{\partial V_y}{\partial x}\right]+\frac{\partial}{\partial y}\left[(\mu+\mu_t)\frac{\partial V_y}{\partial y}\right]+\frac{\partial}{\partial z}\left[(\mu+\mu_t)\frac{\partial V_y}{\partial z}\right]+S_{Tx} \quad (2)$$

$$\rho\left(\frac{\partial V_y}{\partial \tau}+V_x\frac{\partial V_y}{\partial x}+V_y\frac{\partial V_y}{\partial y}+V_z\frac{\partial V_y}{\partial z}\right)=-\frac{\partial P}{\partial x}+\frac{\partial}{\partial x}\left[(\mu+\mu_t)\frac{\partial V_y}{\partial x}\right]+\frac{\partial}{\partial y}\left[(\mu+\mu_t)\frac{\partial V_y}{\partial y}\right]+\frac{\partial}{\partial z}\left[(\mu+\mu_t)\frac{\partial V_y}{\partial z}\right]+S_{Ty} \quad (3)$$

$$\rho\left(\frac{\partial V_z}{\partial \tau}+V_x\frac{\partial V_z}{\partial x}+V_y\frac{\partial V_z}{\partial y}+V_z\frac{\partial V_z}{\partial z}\right)=-\frac{\partial P}{\partial x}+\frac{\partial}{\partial x}\left[(\mu+\mu_t)\frac{\partial V_y}{\partial x}\right]+\frac{\partial}{\partial y}\left[(\mu+\mu_t)\frac{\partial V_y}{\partial y}\right]+\frac{\partial}{\partial z}\left[(\mu+\mu_t)\frac{\partial V_y}{\partial z}\right]+S_{Tz} \quad (4)$$

In the literature, the small blade and the cylindrical roughness element were utilized to control the wake flow as vortex generators by several researchers [32-34]. In this current study, both cylindrical and hemispherical round roughness element were employed to both on slant and rear surface of Ahmed Body as shown in Figure 3. While the hemispherical roughness elements have a lower volume and a more straightforward construction than cylindrical roughness elements, they can also create comparable small-scale coherent vortices. According to their locations and shapes, those different roughness elements were configurated as V_1, V_2, V_3 and V_4. Apart from vortex generators, the deflector configurations were attached the leading part of slant surface, and they were referred as V_5, V_6 and V_7.

Configuration	Technical sketch	Solid model
V_1	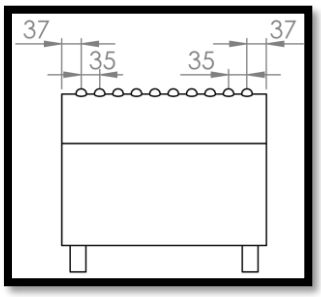	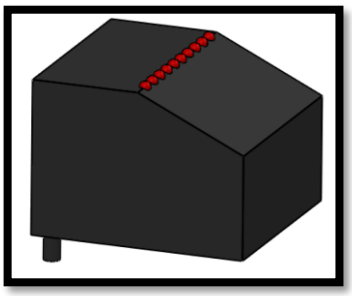
V_2	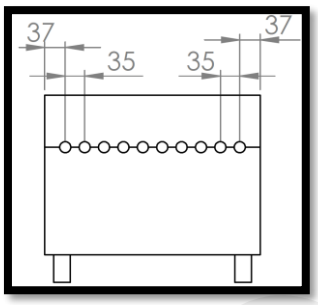	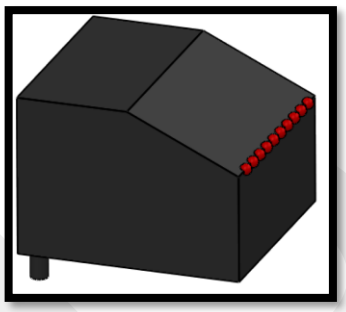
V_3	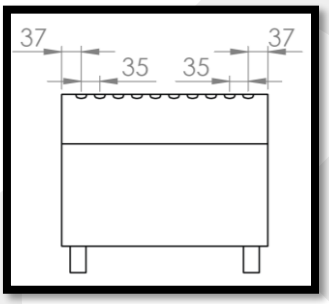	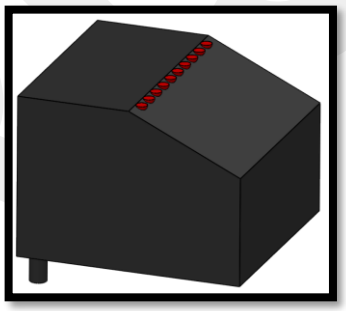
V_4	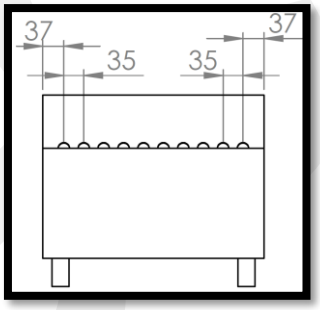	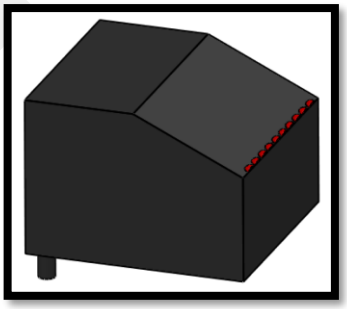
V_5	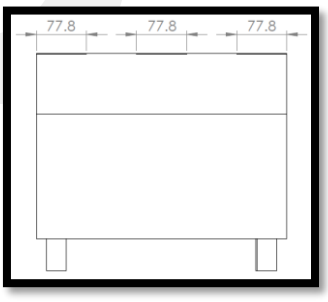	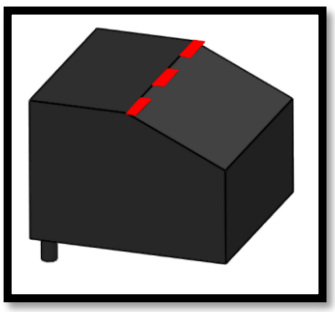

Figure 3. The location of flow controllers on slant surface of Ahmed Body, dimensions in mm (Akış kontrolörlerinin Ahmed Gövdenin eğimli yüzeyindeki konumu, mm cinsinde boyutlar)

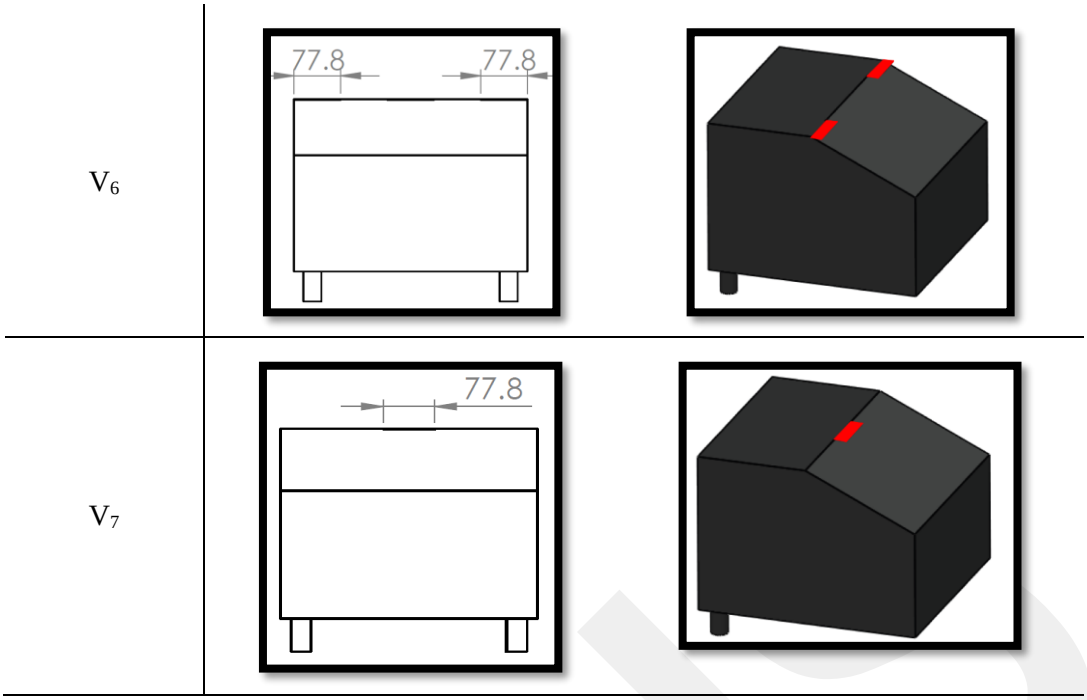

Continuation of Figure 3 (Şekil 3'ün devamı)

2.2. Numerical Method (Sayısal Yöntem)

The mesh structure is one of the key elements in numerical techniques that determines the accuracy of the answer. It plays a direct role in the accuracy of the solution. In this current study, FloEFD software was utilized for numerical analysis. In FloEFD software, the program organizes the mesh structure with its own algorithm and obtains results that are almost independent from the network [35]. As technically speaking, the rectangular computational domain is constructed automatically (but can also be altered manually) to contain the solid body and have boundary planes orthogonal to the Cartesian coordinate system's given axes. Following that, the computational mesh is built in multiple steps. To begin, a simple mesh is created. The computational domain is separated into slices by the basic mesh planes, which are obviously orthogonal to the Cartesian coordinate system axes. The basic mesh cells intersecting the solid/fluid interface are then uniformly split into smaller cells in order to capture the solid/fluid interface with mesh cells of the appropriate size (relative to the basic mesh cells). The solutions were completed in steady-state utilizing the SIMPLE algorithm scheme for pressure-velocity coupling, the least square cell-based approach for gradient, and the second-order upwind method for all other parameters on spatial discretization. Concerning the measure of distance from the first grid cell, y^+ value was about 1. The solutions converged as all residuals reached to 10^{-5}.

Analyzes can be performed without the need for geometry editing in FloEFD software, whereas CFD software users need to prepare the geometry for analysis before solving at different software. The results of the program are compared with other software as well as experimental results in the literature and acceptable results are ensured. The different numerical models were adopted to investigate three-dimensional flow in previous study of the current authors [36]. In this current study, k-Ɛ was selected as the turbulence model for simulations. A separate model specific to the program was created as a result of making arrangements with the experimental data on the standard k-Ɛ model, which is also found in other CFD software in the program. The contact surfaces of the wheels of the Ahmed Body are defined as walls. Velocity is defined separately for each case in the X direction as vector. In Figure 4, the image of the network structure obtained from the software was presented.

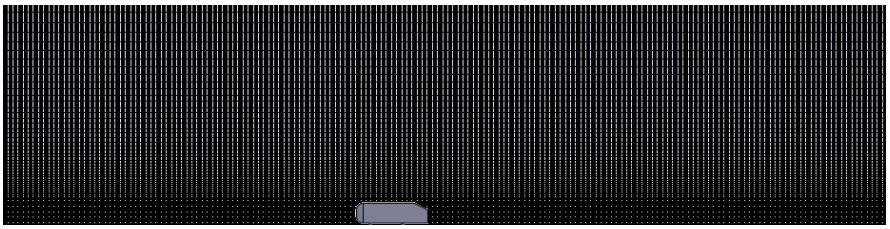

Figure 4. Grid and mesh structures used in the current study (Mevcut çalışmada kullanılan grid ve ağ yapıları)

In addition to the flow analyzes performed in this current study, the aerodynamic drag force created on the Ahmed Body by the flow events was also investigated. In this context, the drag coefficient (C_D) data for the different speeds of the Ahmed Body of all configurations were found with the following equation:

$$C_D = \frac{F_D}{0.5\,\rho\,V^2 A} \tag{5}$$

where F_D, ρ, V and A indicated the aerodynamic drag force, air density, the velocity and projection area of Ahmed Body, respectively. The density is 1.15 m/s^2 and the area is 8.5 m^2. As pointed out before, velocity was 40 m/s.

3. RESULTS (SONUÇLAR)

In this part, the results of velocity graphs, turbulence distribution contours and drag coefficients of the Ahmed Body obtained from the numerical simulation will be discussed. Additionally, three-dimensional contours will be created, and streamlines will be investigated to better understand the flow structures occurring in the front and rear of the Ahmed Body.

3.1. Velocity Distributions (Hız Dağılımları)

Turbulence statistics, Reynolds stress and velocity distributions play crucial roles in the fluid mechanics of understanding the flow phenomena [37-45]. The results of velocity distribution around the Ahmet Body were illustrated in Figure 5. For the baseline model, the velocity decreased at the wake of the body demonstrated as blue region. In particular, it was clearly pointed out that there was huge velocity deficit at the slant surface of the body when VG and deflector were utilized for V_1, V_5 and V_7 configurations. Those flow controllers caused the flow to separate at front of the slant surface. Then, the separated flow reattached the rear part of the body, resulting in presence a huge wake region. Furthermore, there was a longitudinal vortex located at the center of wake region. It was seen that those flow structures were comparatively broaden than other configurations. Apart from those tips, the length of wake region was also taller than other configurations. It was obviously foreseen that V_1, V_5 and V_7 configurations exhibited more dominant role on velocity distribution from slant surface to wake region of Ahmed Body.

3.2. Turbulence Intensities (Türbülans Yoğunlukları)

In aerodynamic literature, the following definitions describe the turbulence intensity, also known as turbulence level:

$$I = \frac{u'}{U} \tag{6}$$

$$u' = \sqrt{\frac{1}{3}(u'^2_x + u'^2_y + u'^2_z)} \tag{7}$$

where u' was the root mean square of the turbulent velocity fluctuations and U is the mean velocity. In Figure 6, the distribution of turbulence intensity was demonstrated for different configurations. One could observe that the turbulence intensity zone at the wake region of the Ahmed Body exactly corresponded to velocity contribution contours. It was clearly seen that there was a shape transition between turbulence intensity contours when different flow control configurations were applied. As discussed at velocity distribution contours, higher turbulence intensity regions were observed at the slant surface and wake region for V_1, V_5 and V_7 configurations. The flow controllers at those configurations caused the flow to be energized, resulting in existing more turbulent velocity fluctuations. Another observation that could be drawn from Figure 6 was that wake shape of Ahmed Body was obviously distinguishable. As a matter of fact, the wake shapes belonging to the V_1, V_5 and V_7 configurations were larger than the other configurations. It spread out more along the flow velocity. It clearly depicted that the turbulence intensity affected more region at the wake part as those configurations were employed.

Configuration	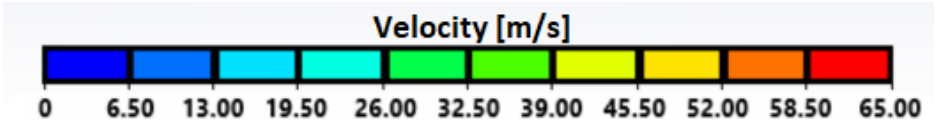
Baseline	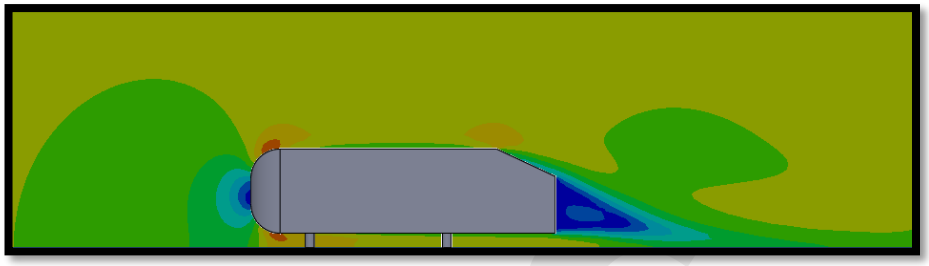
V_1	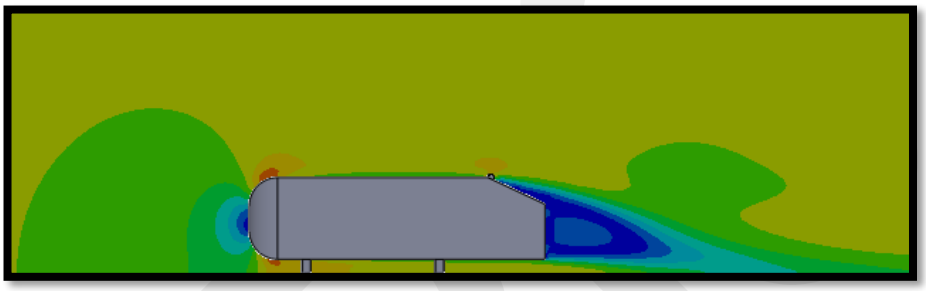
V_2	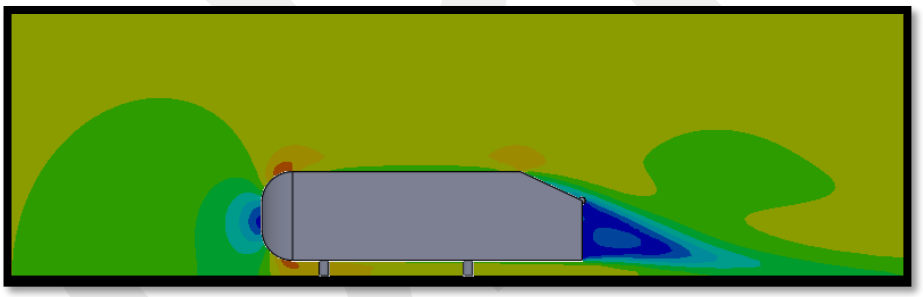
V_3	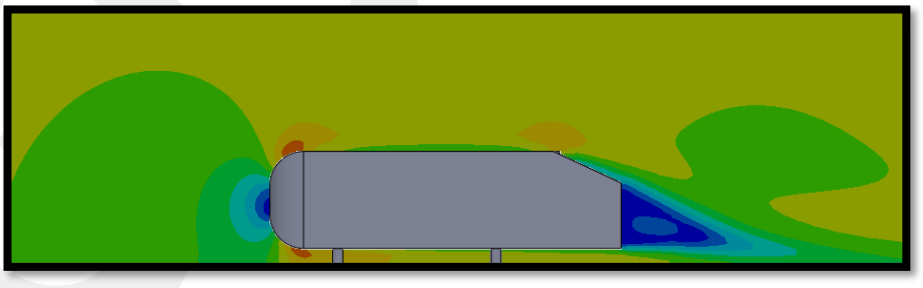
V_4	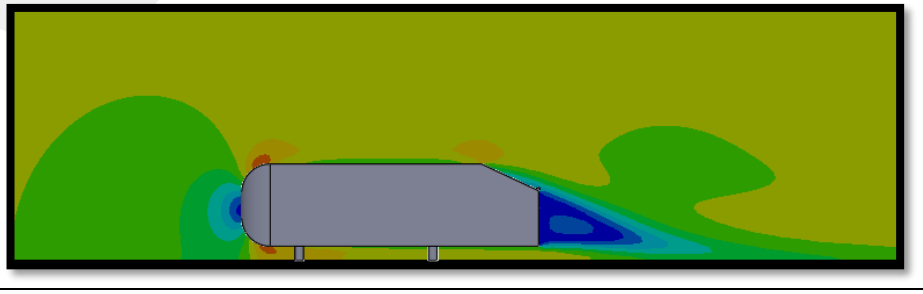

Figure 5. Velocity distribution for various configurations (Çeşitli konfigürasyonlar için hız dağılımı)

V_5	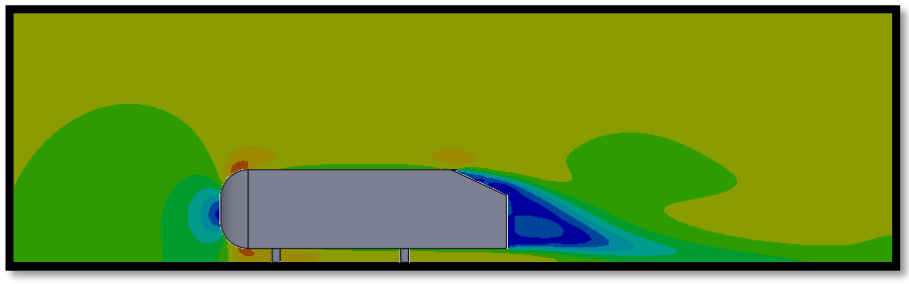
V_6	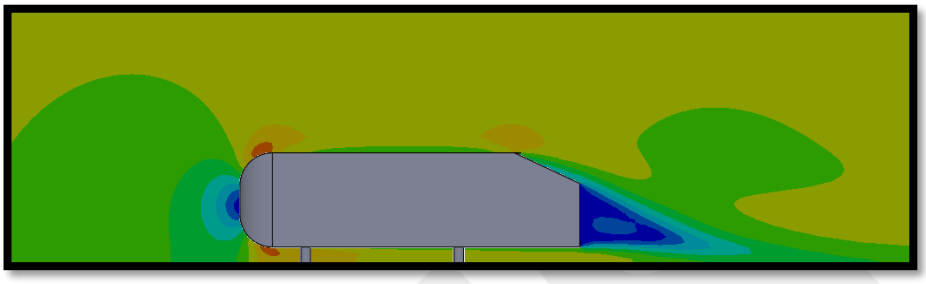
V_7	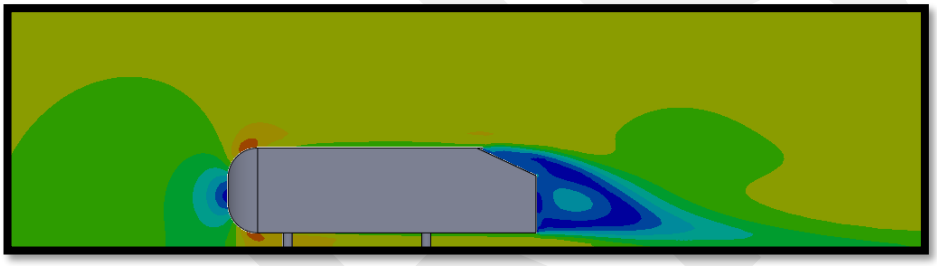

Continuation of Figure 5 (Şekil 5'in devamı)

Configuration	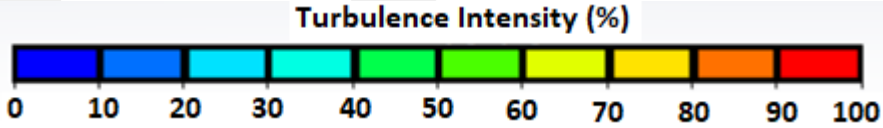
Baseline	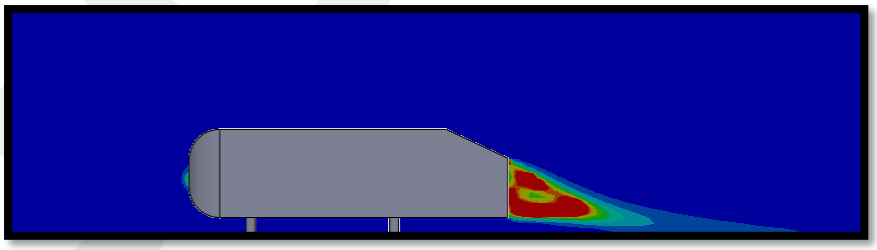
V_1	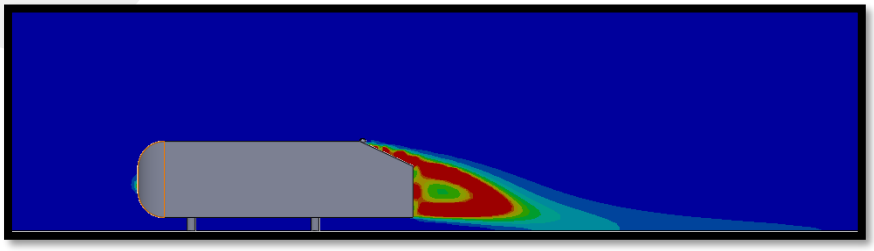

Figure 6. Turbulence intensity distribution for various configurations (Çeşitli konfigürasyonlar için türbülans yoğunluğu dağılımı)

V_2	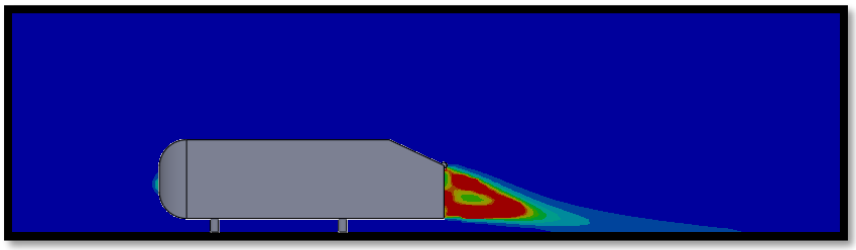
V_3	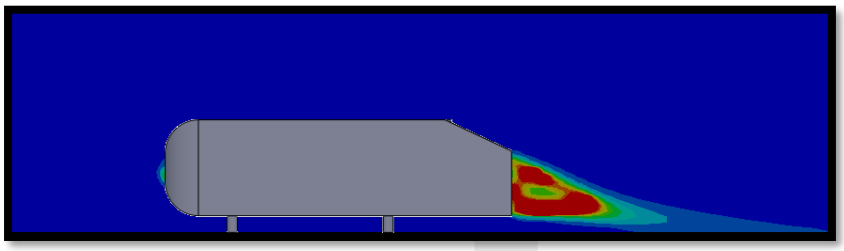
V_4	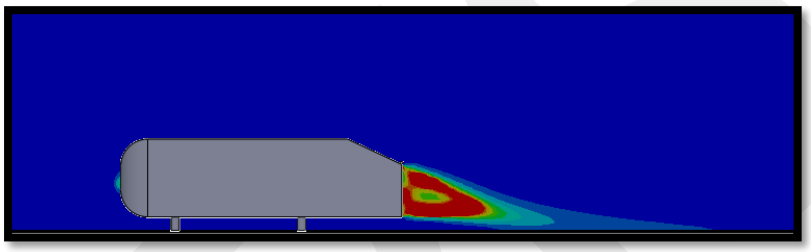
V_5	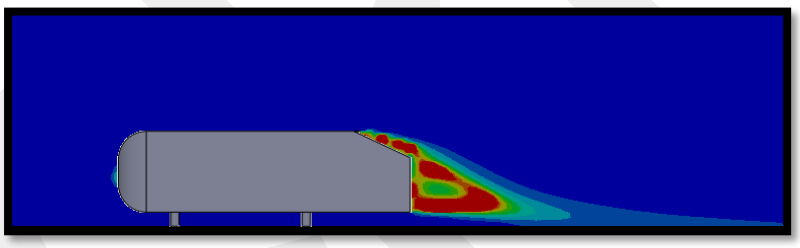
V_6	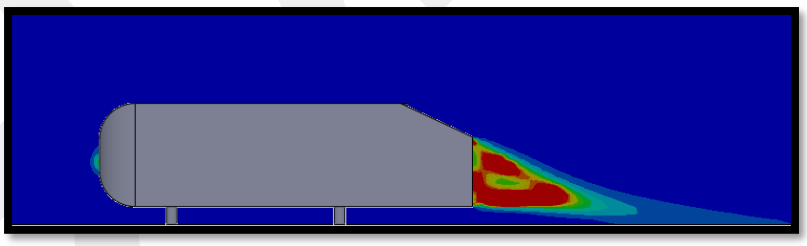
V_7	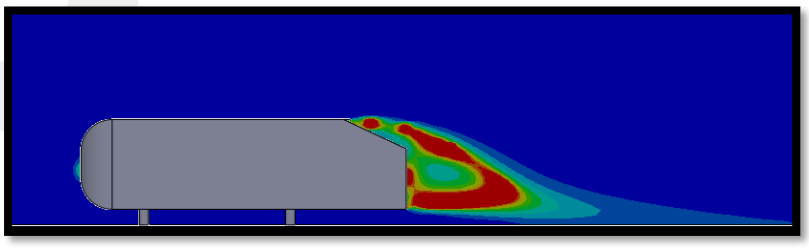

Continuation of Figure 6 (Şekil 6'nın devamı)

3.3. Flow Topologies and Streamline Contours
(Akış Topolojileri ve Akım Çizgisi Konturları)

To better clarify the velocity and turbulence intensity contours, the streamlines images of baseline models belonging to the Ahmed Body presented by current study and the study of Kamacı and Kaya [46] were demonstrated in Figure 7. In particular, as focus on the wake part of Ahmed body for both images, a main recirculation vortex

occurred, indicating that a well harmony appeared at two results under the same conditions.

For all images of current study, the images were focused on the wake region of Ahmed Body to see how the proposed flow controllers affected the region and which type of flow topology occurred. For baseline model in Figure 8, it was clearly seen that there was flow recirculation at the center of wake region. I was most probably occurred due to the flow separation at the slant surface. Moreover, tip vortices occurred at each tip of slant surface, and those flow structures moved along the flow direction by increasing its intensity region. For the flow control configurations, it was clearly understood that the flow structures at the wake changed enormously. Related to the V_1 configuration, the flow was energized much more when the sphere shape flow controller at the front part of slant surface was employed.

Also, circulation region at the near wake bigger than other configurations. Related to the V_2 configuration, the sphere shape flow controller at the rear part of slant surface also affected the flow structure at the wake. However, the size of circulation region at the near wake was less than those occurred configuration of V_1. Additionally, it was accumulated towards to the rear part of the slant surface, resulting in existing distinguishable two zones. Another observation could be seen that the tip vortices belonging to the baseline and V_2 configurations were relatively regular than those occurred at V_1 configuration. Apart from the streamline contours, the vector contours were also important and reliable in terms of explaining flow topology of wake and slant region of Ahmed Body as illustrated in Figure 9. As mentioned in study performed by Yang et al. [47], utilizing passive flow controllers on slant surface caused the small vortices to form on that region and those structures suppressed the flow separation of formation of laminar separation bubble, resulting in presence less drag forces at Ahmed Body. V_1 and V_2 configurations clearly pointed out that different velocity regions existed around the Ahmed Body. This inherently ensured the various pressure regions to form at the same regions. It was foreseen that the pressure deficit in those regions clearly indicated the presence of less drag forces for the Ahmed Body.

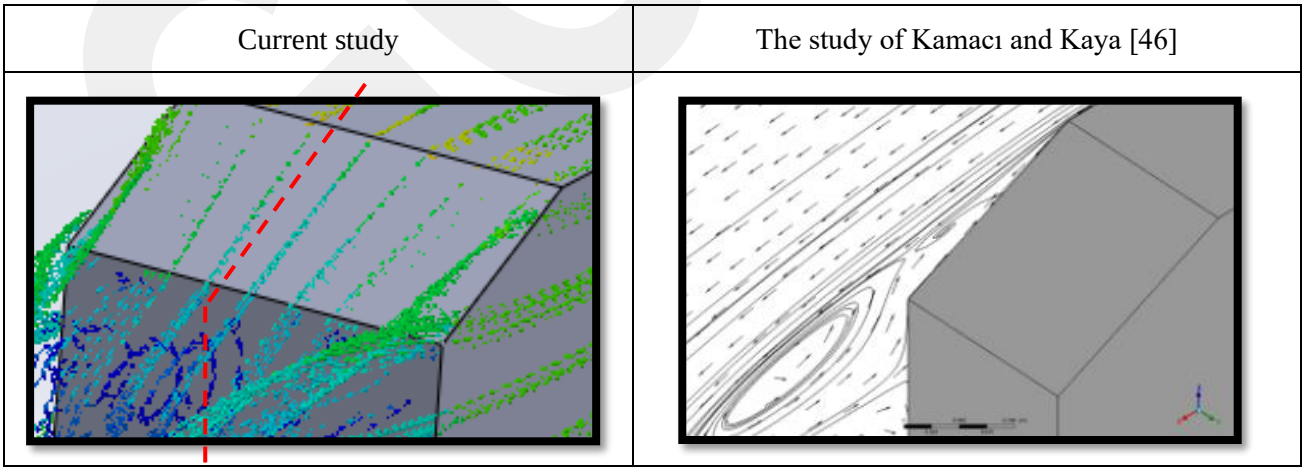

Figure 7. Streamline contours for baseline models at 40 m/s (40 m/s'de temel modeller için akım çizgisi konturları)

Configuration	Top view	3D view
Baseline	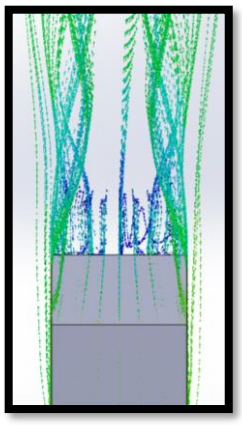	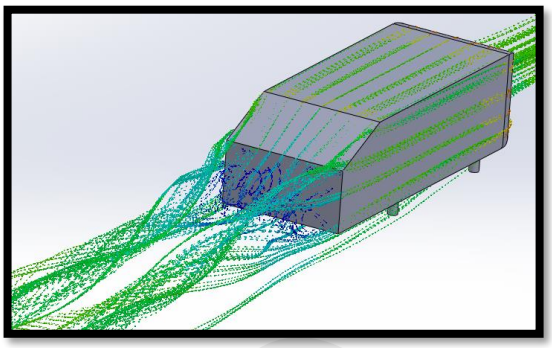
V_1	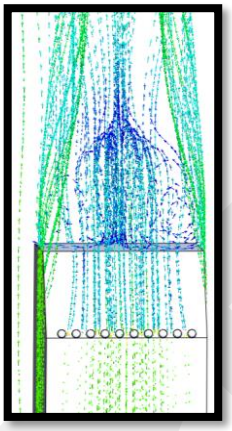	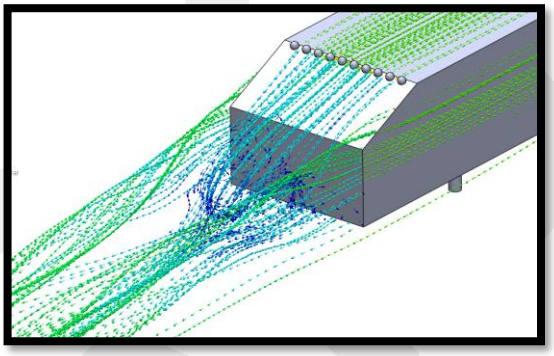
V_2		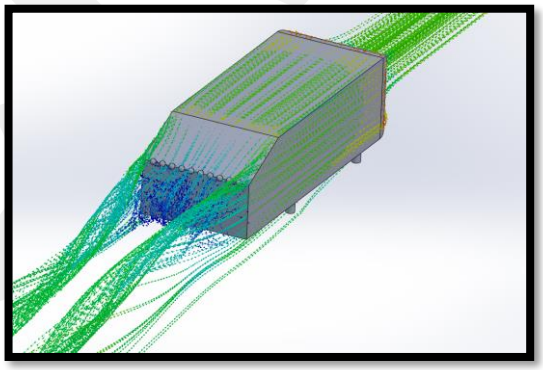

Figure 8. Streamlines for various configurations (Çeşitli konfigürasyonları için akım çizgileri)

Configuration	Top view
Baseline	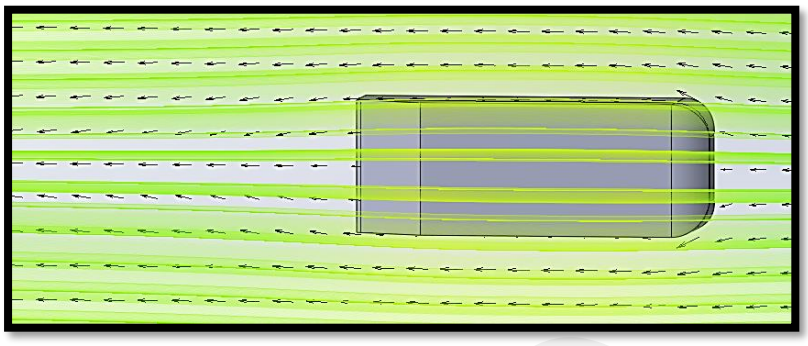
V_1	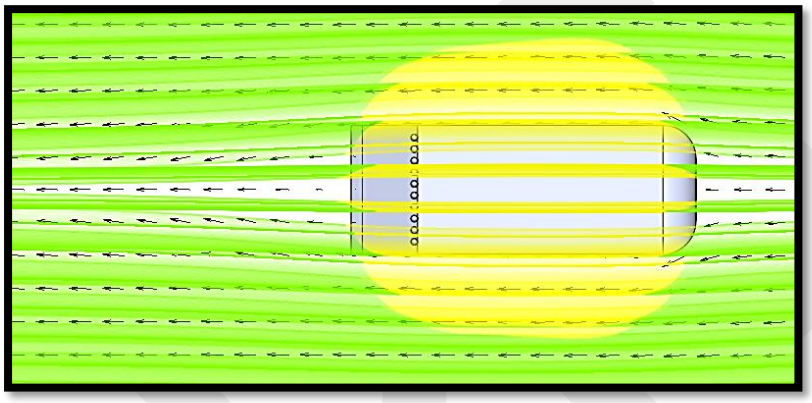
V_2	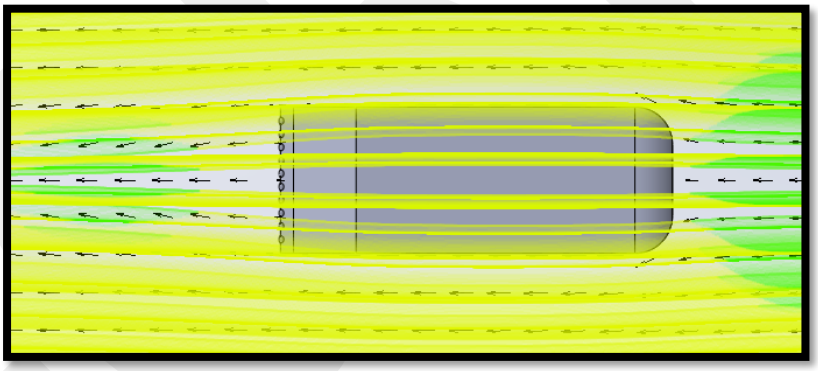

Figure 9. The flow topology of wake and slant region of Ahmed Body (Ahmed Gövdesinin iz ve eğik bölgesinin akış topolojisi)

3.4. Aerodynamic Drag Coefficient (Aerodinamik Sürükleme Katsayısı)

The results of drag coefficients belonging to all configurations at 40 m/s were ensured as illustrated in Figure 10. The different drag coefficient results at the same flow velocity presented by Kamacı &Kaya [46] and Yang et al. [47] were also compiled and put the same figure in terms of comparing the results of current study. The first striking observation from the figure is that all result were close to each other. However, the results obtained from FloEFD were relatively less than those obtained from the ANSYS software. Related to the literature results [46-47], C_D value reduced enormously when the flow controllers were employed. The same observations hold for the current study since there was reduction at the C_D value with utilizing flow control techniques. Related to the proposed method of the current study, V_2 configuration exhibited well performance in terms of drag reduction when the sphere shape flow control was applied at the rear part of the slant surface of Ahmed Body. Another critical observation could be drawn when focused on the results of current and Yang's study [47]. Utilizing both FloEFD and ANSYS software revealed that the best performance in term of drag reduction at the Ahmed Body was provided when hemispherical shape flow control method (V_4 configuration) was

implemented at the rear part of the slant surface. This also displayed that the result obtained from different software consisted with each other well.

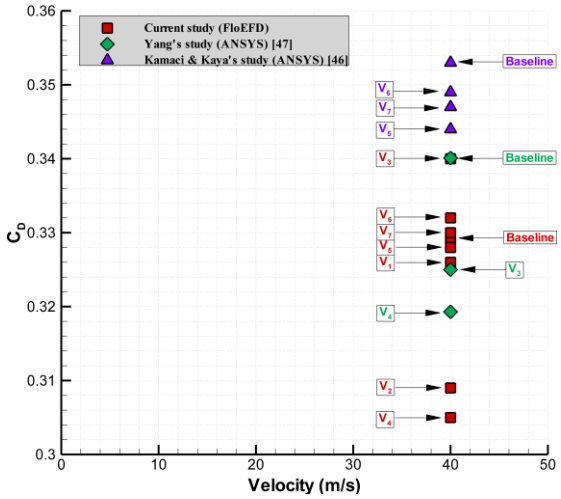

Figure 10. Aerodynamic drag coefficient results from current and literature studies (Güncel ve literatürdeki çalışmalardan elde edilen aerodinamik sürükleme katsayısı sonuçları)

Apart from the aerodynamic drag coefficient results, their percent change to the baseline model was shown in Figure 11. Contrast to Figure 10, the results of only current and Yang's study [47] were provided since they exhibited better solution in terms of reduction in drag. The observation from this figure clearly highlighted that the reduction in drag occurred more when V_4 configuration with hemispherical shape flow control technique was employed at the rear part of slant surface of Ahmed Body. Moreover, the percent variation in drag of V_4 obtained from the FloEFD software was 7%, whilst this value ensured by ANSYS software was 6%.

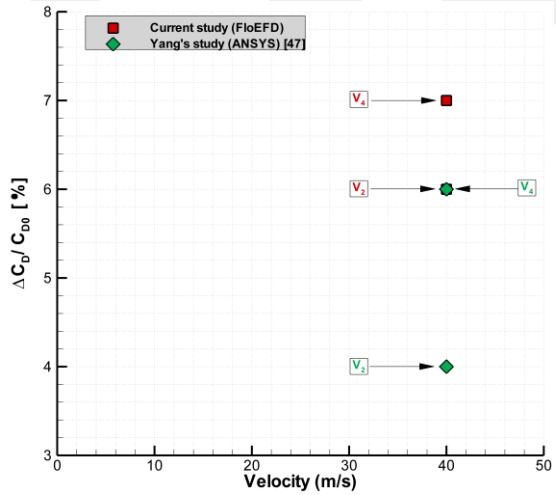

Figure 11. Change in aerodynamic drag coefficient of the Ahmed Body (Ahmed Gövdesinin aerodinamik sürükleme katsayısındaki değişimi)

4. CONCLUSIONS (SONUÇLAR)

This study numerically investigated the flow topology of slant surface and wake region of Ahmed Body as well as its aerodynamic drag coefficients for uncontrolled and controlled cases at 40 m/s. As flow control mechanisms, sphere – hemispherical shape vortex generators as well as deflector were selected. The current results of baseline and flow control configurations were compared with the previously published numerical results in the literature. The critical findings were as follows:

- Among all configurations, it was seen that V_1, V_5 and V_7 influenced the flow structures at the slant surface and wake region of Ahmed Body. When especially focused on velocity and turbulent intensity contours, the flow controllers led the flow to have more energy, resulting in existing small vortices. Those flow structures occurred at the front part of slant surface and moved towards to the wake region of Ahmed Body.

- When observed all aerodynamic drag coefficient results, it was clearly proved that the results of the proposed flow control of this study and V_4 configurations exhibited superior performance in reducing drag coefficient compared to the other configurations. The proposed model of this study (V_2 configuration) reduced the drag about 6%.

- Concerning the different numerical solvers, the results obtained from both the FloEFD and ANSYS software were consistent with each other. Additionally, the percent variation in reducing drag obtained from the FloEFD software was higher than compared to those provided by ANSYS.

This study is expected to shed a lot of light on the bluff body and vehicle aerodynamics. Hereby, the vehicles which are greener and consumed lower fuel can be provided by means of those more effective, innovative flow control techniques.

DECLARATION OF ETHICAL STANDARDS
(ETİK STANDARTLARIN BEYANI)

The author of this article declares that the materials and methods they use in their work do not require ethical committee approval and/or legal-specific permission.

Bu makalenin yazarı çalışmalarında kullandıkları materyal ve yöntemlerin etik kurul izni ve/veya yasal-özel bir izin gerektirmediğini beyan ederler.

AUTHORS' CONTRIBUTIONS (YAZARLARIN KATKILARI)

***Kemal KOCA*:** He analyzed numerical simulation results and performed the writing process.

Sayısal simülasyon sonuçlarını analiz ederek yazma işlemini gerçekleştirdi.

***Mustafa ÖZDEN*:** He performed the literature study and conducted the numerical simulation in detail.

Literatür çalışmasını gerçekleştirdi ve sayısal simülasyonu detaylı bir şekilde gerçekleştirdi.

CONFLICT OF INTEREST (ÇIKAR ÇATIŞMASI)

There is no conflict of interest in this study.

Bu çalışmada herhangi bir çıkar çatışması yoktur.

REFERENCES (KAYNAKLAR)

[1] Ahmed, S. R., Ramm, G., Faltin, G. Some salient features of the time-averaged ground vehicle wake. SAE transactions. 1984; 473-503.

[2] Morel, T. The effect of base slant on the flow pattern and drag of three-dimensional bodies with blunt ends. In Aerodynamic drag mechanisms of bluff bodies and road vehicles, 1978; 191-226.

[3] Zigunov, F., Sellappan, P., Alvi, F. Reynolds number and slant angle effects on the flow over a slanted cylinder afterbody. Journal of Fluid Mechanics. 2020; 893: A11.

[4] Zhang, B. F., Zhou, Y., To, S. Unsteady flow structures around a high-drag Ahmed body. Journal of Fluid Mechanics. 2015; 777: 291-326.

[5] Grandemange, M., Gohlke, M., Cadot, O. Turbulent wake past a three-dimensional blunt body. Part 1. Global modes and bi-stability. Journal of Fluid Mechanics. 2013; 722: 51-84.

[6] Genç, M. S., Koca, K., Demir, H., Açıkel, H. H. Traditional and new types of passive flow control techniques to pave the way for high maneuverability and low structural weight for UAVs and MAVs. Autonomous Vehicles. 2020; 131-160.

[7] Bellman, M., Agarwal, R., Naber, J., Chusak, L. Reducing energy consumption of ground vehicles by active flow control. In Energy Sustainability. 2010; 785-793.

[8] Kourta, A., Leclerc, C. Characterization of synthetic jet actuation with application to Ahmed body wake. Sensors and Actuators A: Physical. 2013; 192: 13-26.

[9] Joseph, P., Amandolese, X., Edouard, C., Aider, J. L. Flow control using MEMS pulsed micro-jets on the Ahmed body. Experiments in fluids. 2013; 54: 1-12.

[10] Zhang, B. F., Liu, K., Zhou, Y., To, S., Tu, J. Y. Active drag reduction of a high-drag Ahmed body based on steady blowing. Journal of Fluid Mechanics. 2018; 856: 351-396.

[11] Brunn, A., Nitsche, W. Active control of turbulent separated flows over slanted surfaces. International Journal of Heat and Fluid Flow. 2006; 27(5): 748-755.

[12] Fourrié, G., Keirsbulck, L., Labraga, L., Gilliéron, P. Bluff-body drag reduction using a deflector. Experiments in Fluids. 2011; 50: 385-395.

[13] Mariotti, A., Buresti, G., Gaggini, G., Salvetti, M. V. (2017). Separation control and drag reduction for boat-tailed axisymmetric bodies through contoured transverse grooves. Journal of Fluid Mechanics. 2017; 832: 514-549.

[14] Aider, J. L., Beaudoin, J. F., Wesfreid, J. E. Drag and lift reduction of a 3D bluff-body using active vortex generators. Experiments in fluids. 2010; 48: 771-789.

[15] Rossitto, G., Sicot, C., Ferrand, V., Borée, J., Harambat, F. Influence of afterbody rounding on the pressure distribution over a fastback vehicle. Experiments in Fluids. 2016; 57: 1-12.

[16] Evrard, A., Cadot, O., Herbert, V., Ricot, D., Vigneron, R., Délery, J. Fluid force and symmetry breaking modes of a 3D bluff body with a base cavity. Journal of Fluids and Structures. 2016; 61: 99-114.

[17] Minguez, M., Pasquetti, R., Serre, E. High-order LES of the flow over a simplified car model: On the influence of the Reynolds number. European Journal of Computational Mechanics/Revue Européenne de Mécanique Numérique. 2009; 18(7-8): 627-646.

[18] Kang, N., Essel, E. E., Roussinova, V., Balachandar, R. Effects of approach flow conditions on the unsteady three-dimensional wake structure of a square-back Ahmed body. Physical Review Fluids. 2021; 6(3): 034613.

[19] Tunay, T., Firat, E., Sahin, B. Experimental investigation of the flow around a simplified ground vehicle under effects of the steady crosswind. International Journal of Heat and Fluid Flow. 2018; 71: 137-152.

[20] Venning, J., McQueen, T., Jacono, D. L., Burton, D., Thompson, M., Sheridan, J. Aspect ratio and the dynamic wake of the Ahmed body. Experimental Thermal and Fluid Science. 2022; 130: 110457.

[21] Essel, E., Das, S., Balachandar, R. Effects of rear angle on the turbulent wake flow between two in-line Ahmed bodies. Atmosphere. 2020; 11(4): 328.

[22] Tunay, T., Yaniktepe, B., Sahin, B. Computational and experimental investigations of the vortical flow structures in the near wake region downstream of the Ahmed vehicle model. Journal of Wind Engineering and Industrial Aerodynamics. 2016; 159: 48-64.

[23] Bruneau, C. H., Mortazavi, I., Gilliéron, P. Passive control around the two-dimensional square back Ahmed body using porous devices. Journal of Fluid Engineering. 2008; 130: 1-12.

[24] Tunay, T., Sahin, B., Akilli, H. Experimental and numerical studies of the flow around the Ahmed body. Wind and Structures. 2013; 17(5): 515-535.

[25] Podvin, B., Pellerin, S., Fraigneau, Y., Evrard, A., Cadot, O. Proper orthogonal decomposition analysis and modelling of the wake deviation behind a squareback Ahmed body. Physical Review Fluids. 2020; 5(6): 064612.

[26] Cadot, O., Evrard, A., Pastur, L. Imperfect supercritical bifurcation in a three-dimensional turbulent wake. Physical Review E. 2015; 91(6): 063005.

[27] Tunay, T., Sahin, B., Ozbolat, V. Effects of rear slant angles on the flow characteristics of Ahmed body. Experimental Thermal and Fluid Science. 2014; 57: 165-176.

[28] Grandemange, M., Cadot, O., Gohlke, M. Reflectional symmetry breaking of the separated flow over three-dimensional bluff bodies. Physical review E. 2012; 86(3): 035302.

[29] Demir, H., Özden, M., Genç, M. S., Çağdaş, M. Numerical investigation of flow on NACA4412 aerofoil with different aspect ratios. In EPJ Web of Conferences. 2016; 114: 02016.

[30] Özden, M., Genç, M. S., Koca, K. Investigation of the effect of hidden vortex generator-flap integrated mechanism revealed in low velocities on wind turbine blade flow. Energy Conversion and Management. 2023; 287: 117107.

[31] Özden, M., Koca, K. Öndeki Aracın Akışına Maruz Kalan Otobüsün Üzerinde Oluşan Aerodinamik Etkinin Sayısal Olarak İncelenmesi. Erciyes Üniversitesi Fen Bilimleri Enstitüsü Fen Bilimleri Dergisi. 2023; 39(1): 116-125.

[32] Özden, M., Genç, M. S., Koca, K. Passive Flow Control Application Using Single and Double Vortex Generator on S809 Wind Turbine Airfoil. Energies. 2023; 16(14): 5339.

[33] Genc, M. S., Koca, K., Acikel, H. H. Investigation of pre-stall flow control on wind turbine blade airfoil using roughness element. Energy. 2019; 176: 320-334.

[34] Pujals, G., Depardon, S., Cossu, C. Drag reduction of a 3D bluff body using coherent streamwise streaks. Experiments in fluids. 2010; 49: 1085-1094.

[35] User guide of FloEFD, Siemens Digital Industries Software, SIEMENS, https://plm.sw.siemens.com/en-US/simcenter/fluids-thermal-simulation/floefd/

[36] Karasu, İ., Özden, M., Genç, M. S. Performance assessment of transition models for three-dimensional flow over NACA4412 wings at low Reynolds numbers. Journal of Fluids Engineering. 2018; 140(12): 121102.

[37] Koca, K., Genc, M. S., Veerasamy, D., Özden, M. Experimental flow control investigation over suction surface of turbine blade with local surface passive oscillation. Ocean Engineering. 2022; 266: 113024.

[38] Genç, M. S., Özkan, G., Özden, M., Kırış, M. S., Yıldız, R. Interaction of tip vortex and laminar separation bubble over wings with different aspect ratios under low Reynolds numbers. Proceedings of the Institution of Mechanical Engineers, Part C: Journal of Mechanical Engineering Science. 2018; 232(22): 4019-4037.

[39] Koca, K., Genç, M. S., Ertürk, S. Impact of local flexible membrane on power efficiency stability at wind turbine blade. Renewable Energy. 2022; 197: 1163-1173.

[40] H Demir, MS Genç, An experimental investigation of laminar separation bubble formation on flexible membrane wing, European Journal of Mechanics-B/Fluids. 2017; 65: 326-338.

[41] Genç, M. S., Koca, K., Açıkel, H. H., Özkan, G., Kırış, M. S., Yıldız, R. Flow characteristics over NACA4412 airfoil at low Reynolds number. In EPJ web of conferences. 2016; 114: 02029

[42] Karasu, I., Genc, M. S., Acikel, H. H., Akpolat, M. T. An experimental study on laminar separation bubble and transition over an aerofoil at low Reynolds number. In 30th AIAA applied aerodynamics conference. 2012; 3030.

[43] Koca, K., Genç, M. S., Özkan, R. Mapping of laminar separation bubble and bubble-induced vibrations over a turbine blade at low Reynolds numbers. Ocean Engineering. 2021; 239: 109867.

[44] Koca, K., Genç, M. S., Açıkel, H. H., Çağdaş, M., Bodur, T. M. Identification of flow phenomena over NACA 4412 wind turbine

airfoil at low Reynolds numbers and role of laminar separation bubble on flow evolution. Energy. 2018; 144: 750-764.

[45] Koca, K., Genç, M.S., Açıkel, H.H. Rüzgar Türbini Kanadı Üzerindeki Yüzey Pürüzlülüğü Etkisinin Deneysel İncelenmesi. Çukurova Üniversitesi Mühendislik-Mimarlık Fakültesi Dergisi. 2016; 31(ÖS2): 127-134.

[46] Kamacı, C., Kaya, K. Numerical Investigation of Aerodynamic Properties of Ahmed Body for Different Rear Slanted Surface Configurations. Avrupa Bilim ve Teknoloji Dergisi. 2021; 28: 469-475.

[47] Yang, X., Hu, Y., Gong, Z., Jian, J., Liu, Z. Numerical study of combined drag reduction bases on vortex generators and riblets for the ahmed body using IDDES methodology. Journal of Applied Fluid Mechanics. 2021; 15(1): 193-207.